Computers and Concrete, *Vol.15, No.4 (2015) 643-671*
DOI: http://dx.doi.org/10.12989/cac.2015.15.4.643

Strength deterioration of reinforced concrete column sections subject to pitting

Rita Greco[2a] and Giuseppe Carlo Marano[*1]

[1]*DICATECH, Department of Civil Engineering, Environmental, Territory, Building and Chemical, Technical University of Bari, via Orabona 4 - 70125, Bari -Italy*
[2]*DICAR, Department of civil Engineering and Architecture, Technical University of Bari, via Orabona 4 - 70125, Bari -Italy*

(*Received July 21, 2014, Revised October 4, 2014, Accecped November 15, 2014*)

Abstract. Chloride induced reinforcement corrosion is widely accepted to be the most frequent mechanism causing premature degradation of reinforced concrete members, whose economic and social consequences are growing up continuously. Prevention of these phenomena has a great importance in structural design, and modern Codes and Standards impose prescriptions concerning design details and concrete mix proportion for structures exposed to different external aggressive conditions, grouped in environmental classes. This paper focuses on reinforced concrete column section load carrying capacity degradation over time due to chloride induced steel pitting corrosion. The structural element is considered to be exposed to marine environment and the effects of corrosion are described by the time degradation of the axial-bending interaction diagram. Because chlorides ingress and consequent pitting corrosion propagation are both time-dependent mechanisms, the study adopts a time-variant predictive approach to evaluate residual strength of corroded reinforced concrete columns at different lifetimes. Corrosion initiation and propagation process is modelled by taking into account all the parameters, such as external environmental conditions, concrete mix proportion, concrete cover and so on, which influence the time evolution of the corrosion phenomenon and its effects on the residual strength of reinforced concrete columns sections.

Keywords: pitting corrosion, strength deterioration, diffusion coefficient, surface chloride concentration, concrete structures, marine environment

1. Introduction

Corrosion of reinforcing steel is widely accepted as the main reason of Reinforced Concrete (RC) structures premature deterioration. One of the main sources of corrosion phenomenon is exposition to chloride attack in marine environments and de-icing salts. In these circumstances, RC members may undergo structural strength degradation due to loss of steel rebar cross sectional area and loss of bond between steel and concrete. While the strength reduction of concrete members suffering corrosion can be directly related to the reduction of the rebar area, the effects on stiffness and ductility of the overall structure are associated with complex mechanisms. These include lack of confinement due to corrosion of transversal reinforcements and bond deterioration between reinforcement and surrounding concrete (Ou *et al*. 2010). These combined mechanisms

*Corresponding author, Professor, E-mail: rita.greco@poliba.it

http://www.techno-press.org/?journal=cac&subpage=8 ISSN: 1598-8198 (Print), 1598-818X (Online)

can significantly reduce in long-term local strength and global ductility and modify sensibly the structural performance during lifetime.

Past researches addressed mainly flexural behaviour of concrete beams damaged by corrosion (Mangat and Elgarf 1999; Rodriguez *et al*. 1997; Almusallam *et al*. 1996). These studies analysed the reduction of load carrying capacity and ductility as consequence of reinforcing steel bars corrosion. Relatively limited literature exists on the axial-bending behaviour of RC columns deteriorated by corrosion phenomenon. Tapan (2009) proposed a bridge pier column strength evaluation method that can be adapted into a currently used bridge condition evaluation method. The proposed evaluation method provided a good estimate of the condition and load-carrying capacity of bridge piers that currently cannot be obtained by normal visual surveys. However, evaluation of strength deterioration was obtained simply fixing a corrosion rate (expressed as the percent of the rebar cross sectional area loss), without considering the structural and environmental parameters which affect the corrosion initiation and propagation process. Biondini and Frangopol (2008) developed a probabilistic limit analysis and lifetime prediction of concrete elements in presence of chloride attack. In the study, the diffusion process for a nominal aggressive scenario was considered and time-variant axial-bending interaction diagrams were obtained. The same author (2011) investigated time-variant structural performance of a critical section of a column where plastic hinges are expected to occur during a seismic event, in terms of bending moment versus curvature relationship, assuming a single given environmental chloride concentration.

At present, for design of RC elements in view of special serviceability limit states, modern Codes and Standards (EN 1992-1-1 2004) define all possible sources of RC elements deterioration and group them in environmental classes. For each class different sub-classes are defined in relation to the aggressive level of the degradation source. Then, for each class some rules and limitations are imposed for structural design. These regard mix proportion, materials mechanical properties, working and curing conditions, minimal structural dimensions and so on. In other words, once the sources of the chemical and/or physical attacks have been identified, Technical Codes (EN 1992-1-1 2004) impose to designers specific requirements in projects, typically concerning the minimum concrete cover, the maximum water/cement ratio, the minimum cement content, the crack width limitation, the air content, the cement type, the coating of concrete surface and others. However, no procedure is provided to assess the time decreasing of structural load carrying capacity with corrosion process evolution.

The present study focuses on the evaluation of residual strength of RC columns subject to pitting corrosion in chloride aggressive environments. Because chlorides ingress and consequent pitting corrosion propagation are both time-dependent mechanisms, the study adopts a time-variant predictive approach to evaluate residual strength of corroded columns at different lifetimes. Even if the proposed approach can be developed for all chloride induced corrosion scenarios, the study focuses on marine environments and their corresponding classes, as currently defined by European Standards (EN 1992-1-1 2004)). In more details, the residual strength of RC columns sections designed according to prescriptions of XS exposure classes is evaluated in terms of axial-bending interaction diagram at selected lifetimes. For each XS exposure class, a consistent corrosion initiation and propagation model is developed, taking into account all the relevant factors affecting the corrosion phenomenon. These are the maximum water/cement ratio, minimum cover and minimum cement content prescribed for the specific class, critical chloride concentration, surface chloride concentration characterizing the exposure class and others.

Based on this model, time-variant axial-bending interaction diagrams for columns sections subject to pitting attack in marine environments are obtained, showing structural load carrying capacity reduction over time. The influence of some design parameters is investigated and results are presented to be useful for possible new design prescriptions.

2. Modeling of pitting corrosion

A typical cause of RC elements degradation in aggressive chloride environments is pitting (or localized) steel corrosion. Structural safety consequences of this specific corrosion can be more serious with respect to effects due to other corrosion mechanisms. In fact, pitting generates an iron oxide that is different from rust resulting from uniform corrosion; it presents a lower volume for unit mass; therefore, it is not able to cause the disruption of the concrete cover. Pitting is then considered more dangerous than uniform corrosion damage because it is more difficult to detect and predict. Corrosion products in fact can often cover the pits; moreover, a small, narrow pit with minimal overall metal loss can lead to the failure of an entire structural system.

In particular, salts spray in marine environments and the use of de-icing salts may generate chlorides penetrating the concrete cover and initiating corrosion (Moodi *et al*. 2014). Chlorides from the environment penetrate the concrete, producing a concentration profile characterized by high chloride content at the exterior surface and decreasing content at a growing depth. The chloride content needs to arrive at a critical value to begin the corrosion process on the steel surface. After this starting event, pitting corrosion propagates and induces loss of steel rebar cross-sectional area. This reduction is not the only consequence of the chloride action in RC structural elements. Reinforcing steel bars manifest in fact a degradation of mechanical properties during the corrosion propagation. Even if section loss of reinforcements is the principal effect of corrosion, this may affect structural strength in several ways, such as loss of bond strength, reduction in the concrete cross section due to corrosion induced cracking and spalling. In a deteriorated column, once the cover spalls off and the bond between the reinforcement and concrete is lost, compressed reinforcements are likely to buckle. If the exposed corroded bar length exceeds a critical length, the reinforcement will buckle before reaching its yield capacity. Thus, load-carrying capacity of the deteriorated column will be reduced i.e., calculations using yield strength will no longer be correct. Anyway, in this study only deterioration effects on longitudinal steel reinforcements are considered. This assumption is accepted because pitting corrosion generates an oxide of iron different from the rust as a result of uniform corrosion, with lower volume for unit mass. Therefore, pitting corrosion is less likely to cause the disruption of the concrete cover and the reduction of bond strength around the pit. For the same reason the effects of corrosion of transverse reinforcement is ignored. These assumptions become unacceptable in the case of uniform corrosion, and therefore in this situation other aspects have to be considered, such as loss of bond strength, modification of compression concrete block and corrosion of transverse reinforcement.

2.1 Geometrical and mechanical properties of the corroded bars

Different experimental investigations showed that the maximum pit depth due to pitting corrosion, $P_{\max}$, is greater than the one due to a general corrosion, P_{av}. The pitting factor R is defined as follows:

$$R = \frac{P_{\max}}{P_{av}} > 1 \tag{1}$$

In the literature, different values are reported for the pitting factor *R*. Gonzalez *et al*. (1995) observed that its value varies from 4 to 8 for bars with a diameter of 8 mm and a length of 125 mm. This is in good agreement with Tuutti (1982), who suggested values from 4 to 10 for steel reinforcing bars with diameters of 5 and 10 mm and lengths varying from 150 to 300 mm.
The maximum pit depth in a reinforcing bar is given by:

$$p(\mathrm{t}) = 0.0116 i_{corr} R t \tag{2}$$

In Eq. (2) *p* is in *mm*, i_{corr} is the corrosion rate, expressed as current density in $\mu A / cm^2$ (for steel, 1 $\mu A / cm^2$ $\approx 11.60 \mu A / yr$) *t* is the time (in year) since corrosion initiation time. Vu and Stewart (2000) give the corrosion rate:

$$i^{(1)}{}_{corr} = \frac{3.78\left(1 - w_c\right)^{-1.54}}{c} \tag{3}$$

where w_c is the water/cement ratio and *c* is the depth of the reinforcement (cm).

This is a simplified model for the corrosion rate, as other variables should be considered, such as temperature and concrete humidity. Despite its limits, the corrosion rate expressed by Eq. (3) is used as it is enough accurate, so that it is commonly adopted in literature (Vu and Stewart 2000, Duprat 2007). However, the corrosion rate is not a fixed parameter as its value decreases with time. Duprat (2007) used a decreasing factor of $t^{-0.3}$. In this study, the following law is adopted:

$$i_{corr}(t) = 0.85 i^{(1)}_{corr} t^{-0.29} \tag{4}$$

This expression is adopted by Vu and Stewart (2000).

In order to define the residual area of a steel bar subject to pitting corrosion, the hemispherical-form model represented in Fig. 1 is assumed (Val and Melchers 2000). Through geometrical considerations, it is possible to obtain residual steel bar area for a maximum pit depth $p(t)$ for a bar with diameter D_0:

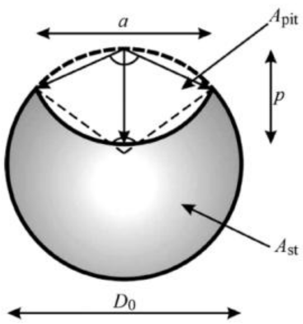

Fig. 1 Pitting corrosion model

$$a(t) = 2p(t)\sqrt{1 - \left(\frac{p(t)}{D_0}\right)} \tag{5}$$

$$A_{pit}(t) = \begin{cases} A_1 + A_2 & if\ p(t) \le \frac{D_0}{\sqrt{2}} \\ \frac{\pi D^2{}_0}{4} - A_1 + A_2 & if\ \frac{D_0}{\sqrt{2}} \le p(t) \le D_0 \\ \frac{\pi D^2{}_0}{4} & if\ p(t) \ge D_0 \end{cases} \tag{6}$$

$$\vartheta_1(t) = 2\arcsin\left(\frac{a(t)}{D_0}\right);\ \vartheta_2(t) = 2\arcsin\left(\frac{a(t)}{2p(t)}\right) \tag{7}$$

$$A_1(t) = 0.5\left[\vartheta_1(t)\left(\frac{D_0}{2}\right)^2 - a(t)\left|\frac{D_0}{2} - \frac{p(t)^2}{D_0}\right|\right]$$
$$A_2(t) = 0.5\left[\vartheta_2(t)p(t)^2 - a(t)\frac{p(t)^2}{D_0}\right] \tag{8}$$

$$A_{st}(t) = \frac{\pi D_0^2}{4} - A_{pit}(t) \tag{9}$$

2.2 Mechanical consequences on steel bars due to the corrosion process

Reinforcements subjected to corrosion attack suffer loss of strength and loss of ductility; thus the original strength of the reinforcement cannot be used for predicting the strength of deteriorated steel bar. The geometry and the modified material properties of corroded reinforcement are used in this study to evaluate the forces acting in the corroded reinforcement in order to obtain time-variant axial-bending interaction diagrams. The residual strength of corroded reinforcing bars was investigated by Du *et al*. (2005). Their test results agreed reasonably well with those obtained under natural corrosion conditions. Therefore, the empirical equation proposed by Du *et al*. (2005) is used to calculate the reduction in the strength of corroded reinforcement:

$$f_y(t) = f_{y0}\left(1 - \alpha_y \frac{A_{pit}(t)}{\frac{\pi D_0^2}{4}}\right) \tag{10}$$

where f_{y0} is the initial yield stress of the non-corroded reinforcing bar. For the coefficient α_y, Du *et al*. (2005) recommend a value of 0.005. This value is adopted also by Stewart and Al-Harthy (2008) and is used in the present study.

3. Corrosion initiation model

The corrosion deterioration process includes corrosion initiation and corrosion propagation. The corrosion initiation time T_i is the period during which the aggressive agents penetrate by means of diffusion into the protective concrete cover or by direct ingress through cracks induced by shrinkage or loading exceeding the cracking capacity of the section, among others. When the threshold level of chloride concentration C_{crit} is reached at the surface of steel bar, the corrosion process starts. This represents the well-known Tuutti's model (1982), widely accepted as the conceptual model for the deterioration of structures (Fig. 2). As depending over time, this model clearly distinguishes an initiation time $\mathrm{T_i}$ followed by a propagation time. The initiation time $\mathrm{T_i}$ refers to the penetration of the aggressive agents into the concrete cover till to a critical concentration at the rebars deep, while the propagation time is related to the evolution of rebars area reduction after corrosion initiation.

Different models for chloride penetration have been proposed and elaborated, and many experimental investigations have been conducted over last decades. However, numerous difficulties still exist because, if the variables involved in the process are known, the physical and chemical mechanisms are less known and, particularly, a no Table indecision with reference to the interactions among all such mechanisms can be noticed. A simplified procedure is based on the hypothesis that the ingress of chlorides is a diffusion process that can modeled by means of Fick's second law, as first realized by Collepardi *et al*. (1972). This is a diffused supposition as adopted by Stewart and Rosowsky (1998). According to this law, the chloride ion content is given by:

$$C(\mathrm{x,t}) = C_s\left[1 - erf\left(\frac{x}{2\sqrt{D_a t}}\right)\right] \tag{11}$$

where $C(x,t)$ is the chloride content (kg/m^3) at distance x (m) from the surface at a generic time instant t (s); C_s is the surface chloride concentration (kg/m^3) and D_a is the apparent diffusion coefficient (m^2/years). Using Eq. (11), it is possible to define the time $\mathrm{T_i}$ for the initiation of steel rebar corrosion with reference to an assigned cover c and a given critical threshold chloride concentration C_{crit}

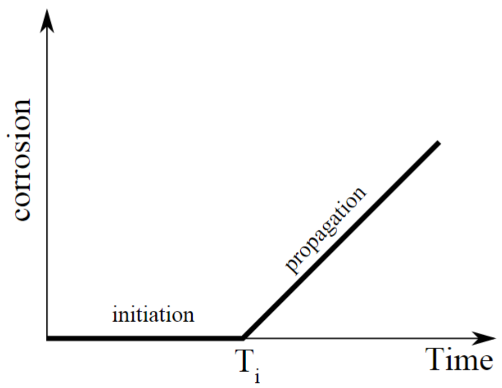

Fig. 2 Tuutti's model (1982)

$$T_i = \left\{ \frac{c^2}{4D_a} \left[erf^{-1} \left(\frac{C_s - C_{crit}}{C_s} \right) \right] \right\}^{-2} \tag{12}$$

3.1 Parameters affecting the diffusion coefficient

Although Eq. (11) and its analytical solution (Eq. (2)) adequately describe the behavior of the concentration of chlorides in the RC structures, the assumption of a constant diffusion coefficient restricts the use of this equation. The chloride diffusion coefficient decreases with time due to several issues such as continued hydration and chloride binding. Laboratory testing (Mangat and Molloy 1994, Maage *et al*. 1999) and some results of existing structures showed that the dependency of the coefficient on the concrete's age obeys a straight line in a double logarithmic coordination system. This meant that the diffusion coefficient could be written as a power function (Tang 1996):

$$D_c(t) = D_{ref} \left(\frac{t_{ref}}{t} \right)^m = K_0 t^{-m} \tag{13}$$

where D_c (t) is the diffusion coefficient at time t; D_{ref} is the diffusion coefficient at the reference time t_{ref} and m is a constant that depends on the mix proportions. K_0 incorporates all the constants and is defined as the effective diffusion coefficient at time t_{ref}. Generally, K_0 is evaluated considering the effective diffusion coefficient at 28 days:

$$D_{ref(28)} = 10^{(-12.06+2.4w_c)} \tag{14}$$

The ageing coefficient m in Eq. (13) is a constant. It depends on some factors such as the type of cement used and the mix proportions, and has been developed to account for the rate of reduction of diffusivity with time. Various empirical relations are available in literature. That proposed by Mangat and Molloy (1994) is widely adopted in literature:

$$m = 2.5w_c - 0.6 \tag{15}$$

The effect of cement content on chloride diffusion of concrete was investigated by various authors. Results showed that cement content has little influence on chloride diffusion of concrete made with similar w_c ratios (Dhir *et al*. 2004).

The empirical constant m can be estimated by interpolation in terms of cement content and w_c ratio. Thus, the values of m can be obtained through the following equation (Rodriguez *et al*. 2013):

$$m = \delta F + \phi \tag{16}$$

where δ and ϕ are empirical coefficients given in terms of w_c:

$$\delta = -0.0015w_c + 0.0034 \tag{17}$$

$$\phi = -0.175w_c + 0.84 \tag{18}$$

F is the concentration of cement (as % of the concrete weight).

For a more realistic prediction of chloride diffusion in concrete, the time dependence of the diffusion coefficient needs to be incorporated into the analysis procedure, thus properly deriving Fick's second law. This model was developed by Mangat and Molloy (1994), leading to the following equation:

$$C(\mathrm{x},\mathrm{t}) = C_s\left[1-erf\left(\frac{x}{2\sqrt{\frac{K_0}{1-m}t^{1-m}}}\right)\right] \tag{19}$$

Using Eq. (19) it is possible to define initiation time T_i with reference to an assigned critical threshold chloride concentration C_{crit}.

$$T_i = \frac{c^2(1-m)}{4K_0}\frac{1}{\left[erf^{-1}\left(\frac{C_{crit}}{C_s}\right)\right]^{\frac{1}{1-m}}} \tag{20}$$

3.2 Critical chloride ion concentration

The critical chloride ion concentration (or chloride concentration threshold level) C_{crit} is one of the main parameters affecting the service life of RC structures. In fact, when a certain amount of chlorides, commonly referred "critical chloride content" C_{crit}, penetrates into the concrete cover at the level of the reinforcement deep, there is a high probability of depassivation. Schiessl and Raupach (1990) stated that the critical chloride ion concentration could be defined as the chloride content that was necessary to sustain local passive film breakdown at the steel depth before the process of corrosion initiation. JSCE (2002) defined the critical value of 1.2 kg/m^3 to initiate reinforcement corrosion. In effect, critical chloride value depends on the roughness of steel surface, concrete properties and the aggressiveness of the environment.

Table 1 Exposure classes related corrosion induced by chlorides from sea water, adapted from (UNI EN 206-1 2006)

Class	Description	Informative examples
XS1	Exposed to airborne salt but not in direct contact with sea water	Structures near to or on the cost
XS2	Permanently submerged	Parts of marine structures
XS3	Tidal, splash and spray zones	Parts of marine structures

Table 2 Critical chloride content C_{crit} for XS exposure classes (Marques *et al*. 2011)

Water/cement ratio	XS1; XS2	XS3
$w_c \leq 0.3$	0.6%	0.5%
$0.3 \leq w_c \leq 0.4$	0.5%	0.4%
$w_c \geq 0.4$	0.4%	0.3%

Table 3 Surface chloride ion concentration in XS exposure classes (Marques *et al*. 2011)

Exposure class	*Nominal value*	*Cov*
XS1	2,31% (weight of binder)	0.10
XS2	6,93% (weight of binder)	0.10
XS3	4,05% (weight of binder)	0.10

Even if the methodology proposed in this study can be applied for all environments the study is carried out considering chloride attack in marine environments and their corresponding classes, according to definitions currently given by the European Standards EN 1992-1-1 (2004) and their Italian version (UNI EN 206-1 2006) (Table 1).

In the following, the environmental exposure class XS (corrosion induced by chlorides from sea water) will be considered. Three subclasses are distinguished: XS1, areas exposed to airborne salt but not in direct contact with sea water; XS2, permanently submerged areas; and XS3, tidal, splash and spray zones. With regard to C_{crit}, the values in Table 2 are adopted in this study according to each exposure class and w_c ratio (Marques *et al*. 2011).

3.3 Surface chloride ion concentration

The surface chloride ion concentration depends on many factors, for example, the distance of the structure from the sea, the region of structure (i.e., atmospheric, tidal, splash, or submerged zones), and concrete properties, the wind speed etc. Several researchers have proposed close-formed solutions for both time independent and dependent surface chloride ion concentration. Costa and Appleton (1999) presented an experimental study where the parameters used in the penetration model were calibrated to allow the prediction of long term chloride content in concrete. In their study, the surface chloride models were considered depending on concrete mix proportion and exposure conditions. The results showed however that the concrete mix does not affect significantly the surface chloride content.

In this study the values listed in Table 3 are adopted for surface chloride concentration in marine exposure classes XS (Marques *et al*. 2011).

In Table 3, nominal values and covariance coefficients of surface chloride ion concentration for each environmental class are furnished. These data are used to define a nominal and a worst environment scenario, respectively: nominal scenario is obtained considering nominal value of chloride surface concentration, while in worst scenario, chloride surface concentration is defined as $\mu + \operatorname{cov} \mu$.

4. Corrosion initiation and propagation model for RC members designed in marine environments

For design of RC elements in view of special serviceability limit states such as corrosion due to chloride penetration, current Technical Codes impose some rules and limitations. These prescriptions regard materials compositions and their mechanical properties, working and curing conditions, minimal structural dimensions and so on. In other words, once the sources of the chemical and/or physical attacks have been identified, Technical Codes impose to designers specific requirements in projects, typically concerning the minimum concrete cover, the maximum water/cement ratio, the minimum cement content, the crack width limitation, the air content, the cement type, the coating of concrete surface and others.

Once the aggressive environment has been fixed, designers can define the maximum water/cement ratio, the strength class, the minimum cement content and the minimum concrete cover, given in Table 4 (UNI EN 206-1 2006). Prescription in Table 4 are applicable for an "assigned expected" lifetime for common structures (50 years), and for Portland cement. For structures whose expected service life is 100 years, a larger minimum concrete cover is specified.

In this study a predictive model to evaluate deterioration of load carrying capacity of columns sections designed in XS exposure classes is developed, obtaining time-variant axial-bending interaction diagrams. The initiation and propagation model is elaborated for each exposure class assigning the admissible minimum values of concrete cover and cement content, and the maximum value of w_c ratio (Table 4). Moreover, critical chloride concentration and chloride surface concentration are assumed according to literature data for the selected class (Tables 2 and 3). It is obvious that the quality of the evaluation depends strongly on input data quality. In case of chloride ingress models, a wide variation in some of involved parameters exists (Shin *et al*. 2011).

Particularly, the surface chloride concentration is one of the less certain parameter (Marano *et al*. 2010, Marano *et al*. 2008) depending for a given class from the exposure conditions, such as the wind speed, the distance from the coast and others. However, also the other parameters involved in the analyzed problem are affected by uncertainty, both those directly involved in the corrosion process (pitting factor, diffusion coefficient, concrete cover, critical ion concentration) and those involved in strength evaluation (materials properties and dimension). To consider the random nature of all parameters would require a full probabilistic approach. This greatly complicates the analysis, which instead has different goals. For this reason, only the uncertainty associated with the determination of C_s is considered in this study, assuming nominal and worst chloride aggressive scenarios. The others parameters are assumed as mean value and therefore the axial-bending interaction diagrams must be considered as in terms of mean.

Table 4 Indicative requirements for concrete structures in chloride aggressive environments, adapted from (EN 206-1, 2006)

Class	Maximum water/cement ratio	Strength class (MPa)	Minimum cement content (kg/m^3)	Minimum concrete cover (mm)
XS1	0.50	C30/37	300	35 (45 mm—100 years)
XS2	0.45	C35/45	320	40(50 mm—100 years)
XS3	0.45	C35/45	340	45(55 mm—100 years)

5. Axial –bending interaction diagram for deteriorated RC columns in XS exposure class

Interaction diagrams for a RC section are generally computed by assuming a series of strain distributions, each corresponding to a particular point of the interaction diagram, and then computing the corresponding values P_{rd} and M_{rd}. Once enough such points have been computed, the results are summarized in an interaction diagram.

A rectangular cross section with symmetric reinforcing steel area $A_s=A_s'$ is considered in this study (Fig. 3). For concrete, the parabola rectangle stress – strain diagram (EN1992-1-1 2004) is adopted with calculus compression strength f_{cd}. The maximum compressive strain is set at 0.0035 for neutral axis internal to the section and varying between 0.0035 and 0.002 for neutral axis external to the section (valid for f_{ck} lower than 50*MPa*, where f_{ck} is the concrete characteristic cube strength). For steel, the stress – strain diagram is described by an elastic perfectly plastic model in both tension and compression, with the following calculus parameters: yielding strength f_{yd} =391,3 *MPa*; elastic modulus E_s=200.000*MPa* (Fig. 4). The location of the neutral axis and the strain in each level of reinforcement are computed from the strain distribution. This information is then used to compute the size of the compression region and the stress in each layer of reinforcement. The forces in the concrete and steel layers are computed by multiplying the stresses by the corresponding areas on which they act. Finally, the calculus resistant axial force P_{rd} is computed by adding forces in concrete and steel, and the calculus resistant bending moment M_{rd} is calculated by adding moments of these forces around section plastic centroid. The cross section of reinforcing bars and yielding strength vary with the time according to Eqs. (9) and (10).

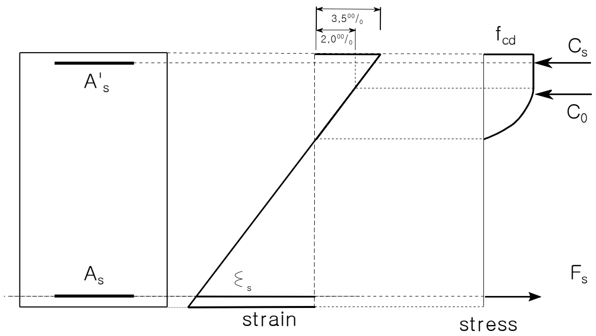

Fig. 3 Rectangular RC section whit symmetric reinforcing steel area: ultimate strain distribution diagram and correspondent resultant forces diagram

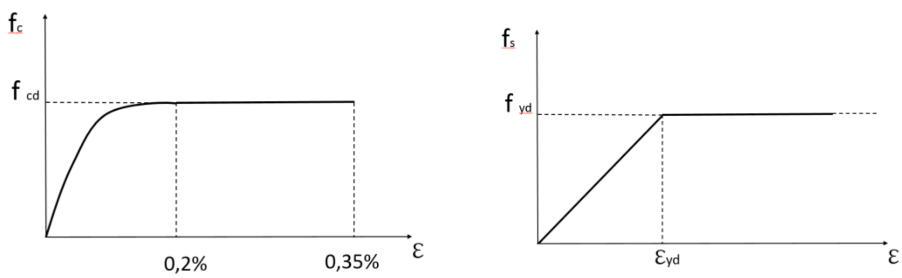

Fig. 4 Concrete and steel calculus stress-strain diagrams

6. Results of the case study using the proposed methodology

In this section, the results of the proposed methodology are shown and then discussed. A RC column with a rectangular section with dimensions b = 30cm and h = 50 cm and symmetric reinforcing steel area is examined. The aim is to investigate the evolution of the axial-bending interaction diagram as consequence of the pitting phenomenon induced by chlorides attack in marine environments. Calculus compression strength of the concrete is assumed f_{cd} = 14,167 *MPa*.

The column cross-section is considered exposed to chloride diffusive attack in XS exposure classes. It is assumed that the structural element has been designed according to the requirements concerning the minimum concrete cover, the maximum water/cement ratio and the minimum cement content given for each class in Table 4 for a 50 years and a 100 years expected lifetime respectively. Axial-bending interaction diagram is evaluated at t = 0 years, t = 50 years, t = 100 years and t = 150 years. Two different situations concerning the aggressive scenario for each exposure class are considered, i.e. a nominal scenario and a worst scenario. In the cases of study, some design parameters are varied with respect to prescriptive limits given in Table 4, in order to investigate their influence on the load carrying capacity of the deteriorated column. Moreover, different diameters are considered in order to investigate the influence on strength deterioration.

All cases of study are specified in Table 5. The results of numerical analyses are provided in Table s 6-9, which furnish the values of ultimate bending at the balanced rupture M_{rdb}, the ultimate bending M_{rd} in the case of simple bending and the ultimate axial force N_{rd} in the case of simple compression. In addition, in Table s 7-9 the loss of steel bars area is furnished at t=50, 100 and 150 years. With regards the percentage loss of steel bars area it should be noted that for the compression bars, this loss will produce not only a reduction of the section strength (evaluated by interaction domains) but also a substantial change on the buckling behavior. Kashani *et al* (2013) have investigated this phenomenon.

Fig. 5 shows time-variant interaction diagrams for the RC column in the XS1 exposure class assuming a nominal aggressive scenario. A low pitting factor (R = 4) is considered. Column has been designed according to prescriptive limits given in Table 4 for a 50 years target lifetime. Reinforcement is made by $A_s = A'_s = 4\Phi_{12}$. Results show that the strength of the column designed for a service life of 50 years decreases over the target lifetime and obvious over increasing lifetimes (100 years and 150 years). This result points out that prescriptive limits concerning the minimum concrete cover, the maximum water/cement ratio and the minimum cement content for the XS1 class don't guarantee that initial load carrying capacity of the column is the same over 50 years. If the ultimate strength corresponding to balanced rupture is considered, the ultimate bending M_{rdb} after 50 years is reduced of 3.65%.

In Fig. 6 the time-variant interaction diagrams are showed in case of the worst aggressive scenario. The strength reduction is practically the same of the previous examined case. A larger chloride surface concentration, in fact, determines only a reduction of the initiation period, and when the corrosion propagates, this is controlled by parameters related to concrete properties and cover. This result shows, therefore, that even in the proposed model there is uncertainty about the aggression scenario, the influence on strength deterioration can be neglected.

Fig. 7 shows time-variant interaction diagrams in case of a larger pitting factor value (R=6). The other data are the same used for Fig. 5. In this case, column strength reduction is greater. For example, after 50 years the reduction of the ultimate bending at the balanced rupture is of 6.5% for R=6 and of the 3,65 % for R=4. These results indicate that even if the reduction of the columns

Table 5 Description of the cases of study

Case of study	Exposure class	A_s	R	w_c	c (mm)	Minimum cement content (kg/m^3)
1 (Fig. 5)	XS1	$A_s = A'_s = 4\Phi_{12}$	4	0.5	35	300
2 (Fig. 6)	XS1	$A_s = A'_s = 4\Phi_{12}$	4	0.5	35	300
3 (Fig. 7)	XS1	$A_s = A'_s = 4\Phi_{12}$	6	0.5	35	300
4 (Fig. 8)	XS1	$A_s = A'_s = 4\Phi_{12}$	4	0.5	45	300
5 (Fig. 9)	XS1	$A_s = A'_s = 6\Phi_{10}$	4	0.5	35	300
6 (Fig. 10)	XS1	$A_s = A'_s = 6\Phi_{10}$	6	0.5	35	300
7 (Fig. 11)	XS1	$A_s = A'_s = 3\Phi_{18}$	6	0.5	35	300
8 (Fig. 12)	XS1	$A_s = A'_s = 4\Phi_{12}$	4	0.45	35	300
9 (Fig. 13)	XS1	$A_s = A'_s = 6\Phi_{10}$	4	0.45	35	300
10 (Fig. 14)	XS1	$A_s = A'_s = 6\Phi_{10}$	6	0.45	35	300
11 (Fig. 15)	XS1	$A_s = A'_s = 6\Phi_{10}$	4	0.45	45	300
12 (Fig. 16)	XS2	$A_s = A'_s = 4\Phi_{12}$	4	0.45	40	320
13 (Fig. 17)	XS2	$A_s = A'_s = 6\Phi_{10}$	6	0.45	40	320
14 (Fig. 18)	XS2	$A_s = A'_s = 6\Phi_{10}$	6	0.45	50	320
15 (Fig. 19)	XS2	$A_s = A'_s = 6\Phi_{10}$	6	0.40	50	320
16 (Fig. 20)	XS3	$A_s = A'_s = 4\Phi_{12}$	4	0.45	45	340
17 (Fig. 21)	XS3	$A_s = A'_s = 4\Phi_{12}$	4	0.45	55	340
18 (Fig. 22)	XS3	$A_s = A'_s = 6\Phi_{10}$	6	0.45	45	340

strength after 50 years seems low (in case of Fig. 5), in effect this strength reduction has been evaluated assuming a low value of the pitting factor (which varies from 4 to 10). When this parameter increases, a larger reduction of the column strength takes place.

In Fig. 8 interaction diagrams are plotted for the nominal scenario and assuming the minimum cover for 100 years target lifetime. It is noted that prescribed limits for 100 years lifetime guarantee that the initial performances in terms of load carrying capacity of the column are almost the same throughout the first 50 years in this exposure class. After 100 years the column strength shows a reduction.

In Fig. 9 the interaction diagrams are obtained for the nominal scenario, 50 years prescribed limits as in Fig. 5, but considering the same amount of steel realized with $A_s = A'_s = 6\Phi_{10}$.

Results point out that the bar diameter influences the deterioration of the strength over the structure lifetime. In fact, when the pitting corrosion propagates after the initiation period, the effects of steel reinforcement corrosion are more significant for small bar diameters, as expected, since the percentage of bar area loss is larger. Thus, in a corroding structure few large diameter bars seem to be apparently safer than a higher number of small diameter bars. However, the loss of steel mass should be compared with the other effects of corrosion to explain the role of the bar diameter on the lifetime deterioration mechanism. In fact, in case of presence of corrosion products, also compression strength deterioration should be taken into account. Reduction of

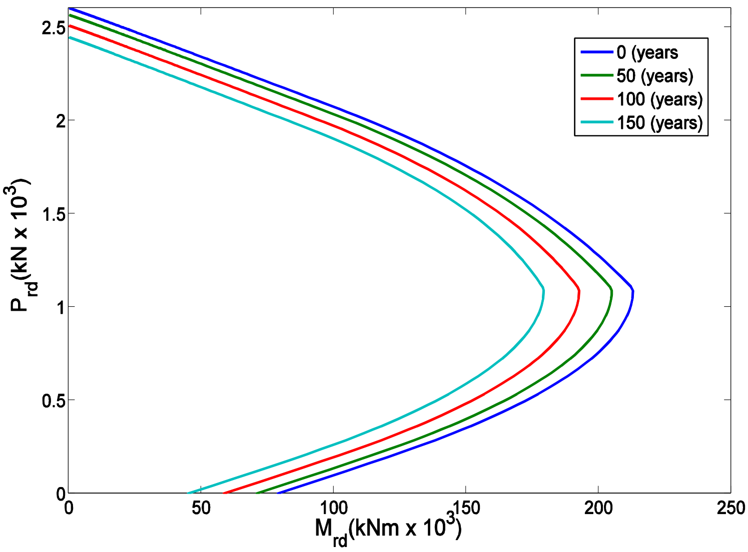

Case 1

XS1; w_c=0.5; c=35 (mm)

cement content = 300(kg/m^3)

$A_s = A'_s = 4\Phi_{12}$

R=4

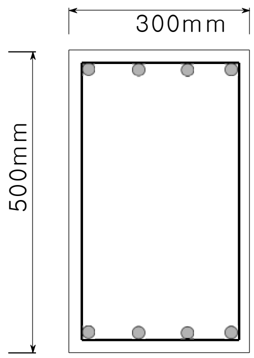

Fig. 5 Time -variant interaction diagrams for XS1 class. A nominal scenario is assumed with prescriptive limits given for 50 years expected life (case 1)

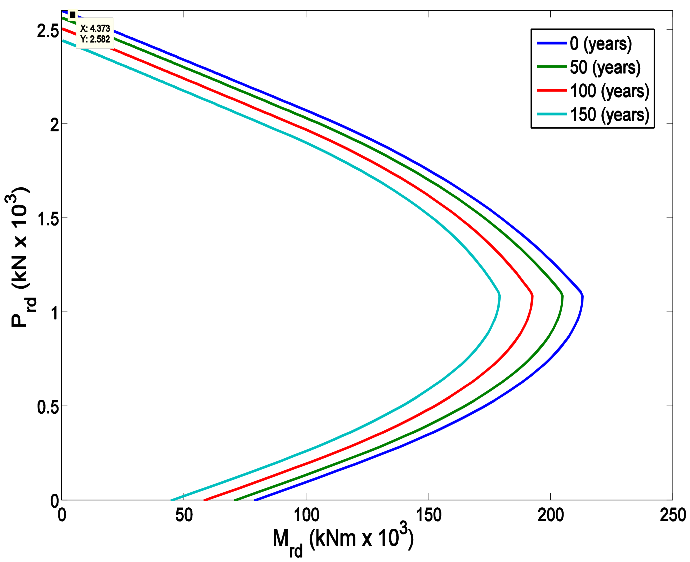

Case 2

XS1; w_c=0.5; c=35 (mm)

cement content = 300(kg/m^3)

$A_s = A'_s = 4\Phi_{12}$

R=4

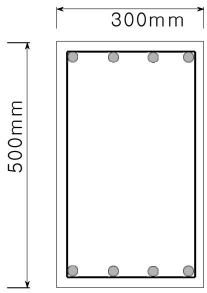

Fig. 6 Time -variant interaction diagrams for XS1 class. A worst scenario is assumed with prescriptive limits for 50 years expected life (case 2)

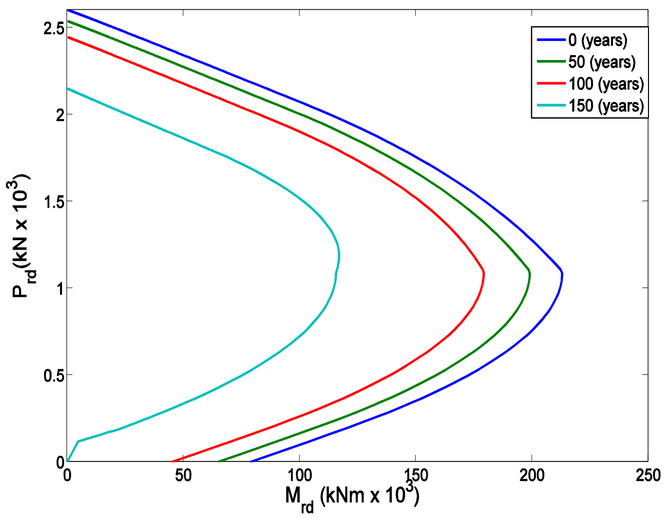

Case 3

XS1; w_c=0.5; c=35 (mm)

cement content = 300(kg/m^3)

$A_s = A'_s = 4\Phi_{12}$

R=6

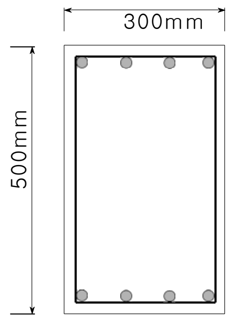

Fig. 7 Time -variant interaction diagrams for XS1 class. A nominal scenario is assumed with prescriptive limits for 50 years expected life (case 3)

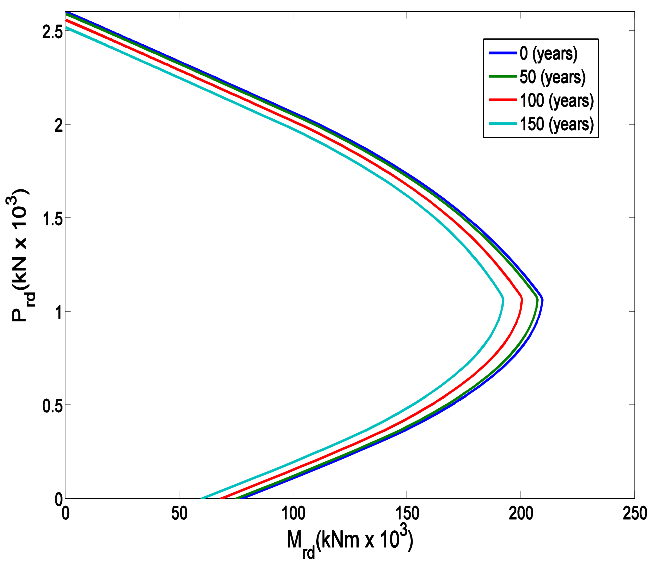

Case 4

XS1; w_c=0.5; c=45 (mm)

cement content =300 (kg/m^3)

$A_s = A'_s = 4\Phi_{12}$

R=4

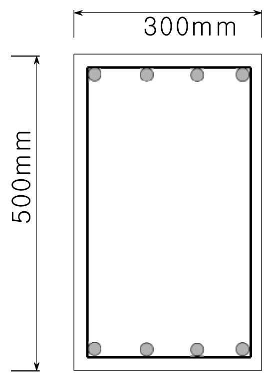

Fig. 8 Time -variant interaction diagrams for XS1 class. A nominal scenario is assumed with prescriptive limits for 100 years expected life (case 4)

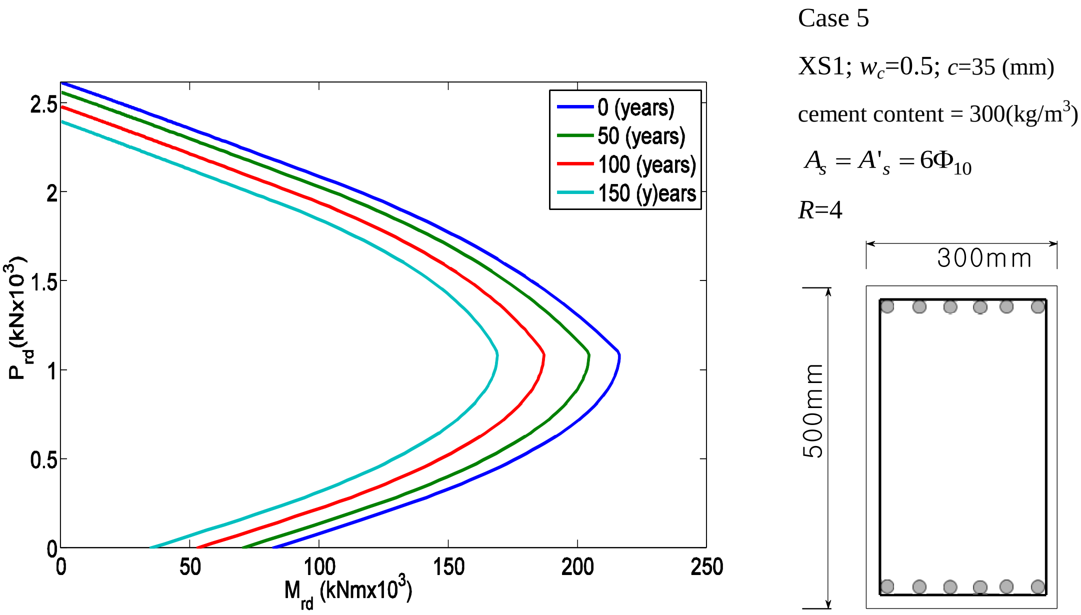

Fig. 9 Time -variant interaction diagrams for XS1 class. A nominal scenario is assumed with prescriptive limits for 50 years expected life (case 5)

concrete strength is greater for larger diameters since the width of cracks increases with larger diameters. With this regard, small bar diameters seem therefore preferable than large bar diameters to avoid splitting cracks and spalling of concrete cover and, in this way, to limit the chloride ingress into concrete. However, these considerations about concrete strength deterioration are irrelevant in case of pitting corrosion for the reasons previous explained and therefore one can conclude that in structures corroded by pitting phenomenon, few large diameter bars can be considered safer than a higher number of small diameter bars.

In Fig. 10 the interaction diagrams are obtained for the same conditions of Fig. 9 and assuming a pitting factor R = 6. One can immediately observe that the reduction of the strength is more serious with respect to the case of R = 4 and therefore one can conclude that when one presumes that the pitting factor can assume high values, one must give great attention to the choice of the bars diameter. Fig. 11 shows the strength deterioration for R = 6 and $A_s = A'_s = 3\Phi_{18}$ A lower decrease of the column strength over the time is noticed with respect to the case analyzed in Fig. 7. In Fig. 12 interaction diagrams have been evaluated for a column designed with prescriptive limits for 50 years lifetime in XS1 exposure class, but the w_c ratio is assumed 0.45.

The comparison with interaction diagrams of Fig. 5 points out that w_c influences the strength deterioration of the column. In fact, whereas for w_c =0.5 after 50 and 100 years M_{rd} at the balanced rupture is decreased respectively of the 3.65% and 9,53%, reducing w_c, M_{rd} after 50 and 100 years is reduced of the 2,3% and 7,1%.

The importance of reducing the maximum w_c is more evident in case of smaller diameter (fig 13) and higher pitting factor (Fig. 14). In fact, comparing Fig. 13 with Fig. 9 immediately one observes that the strength deterioration is lower for a smaller value of w_c.

Case 6

XS1; w_c=0.5; c= 35(mm)

cement content = 300(kg/m^3)

$A_s = A'_s = 6\Phi_{10}$

R=6

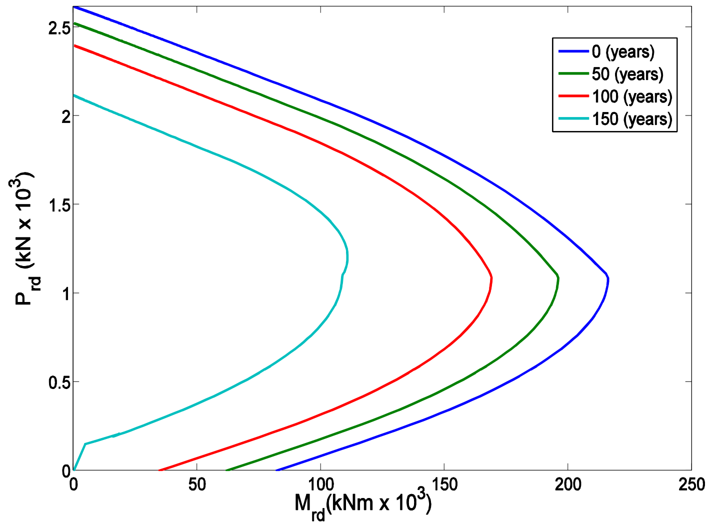

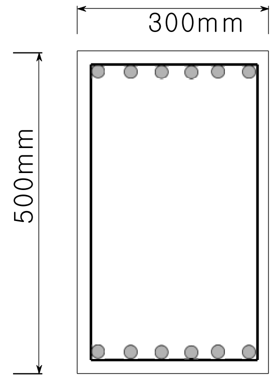

Fig. 10 Time -variant interaction diagrams for XS1 class. A nominal scenario is assumed with prescriptive limits for 50 years expected life (case 6)

Case 7

XS1; w_c=0.5; c=35 (mm)

cement content =300 (kg/m^3)

$A_s = A'_s = 3\Phi_{18}$

R=6

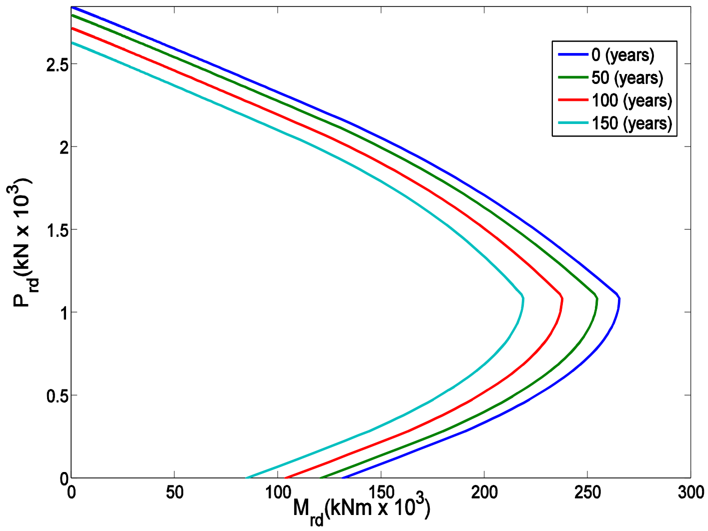

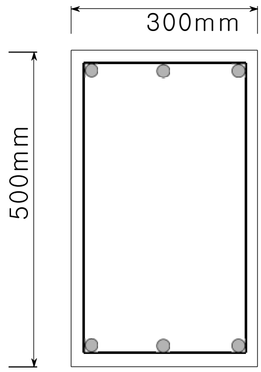

Fig. 11 Time -variant interaction diagrams for XS1 class. A nominal scenario is assumed with prescriptive limits for 50 years expected life (case 7)

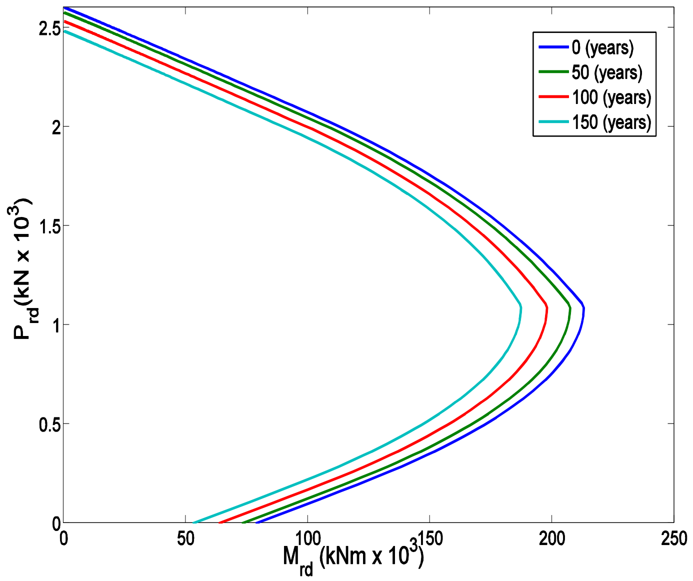

Case 8
XS1; w_c=0.45; c= 35(mm)
cement content = 300(kg/m^3)
$A_s = A'_s = 4\Phi_{12}$
R=4

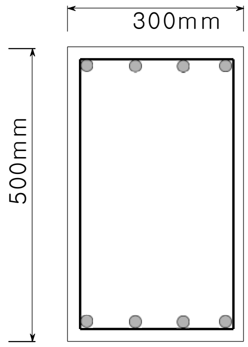

Fig. 12 Time -variant interaction diagrams for XS1 class. A nominal scenario is assumed with prescriptive limits for 50 years expected life, except for w_c, assumed 0.45 (case 8)

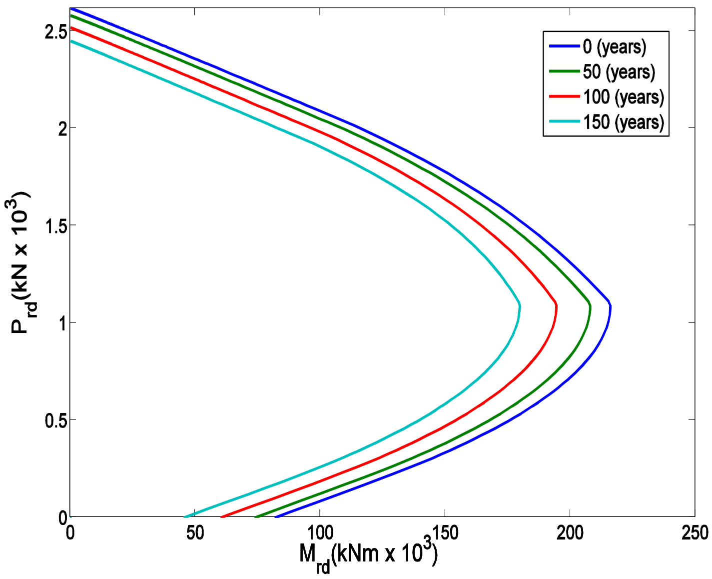

Case 9
XS1; w_c=0.45; c=35 (mm)
cement content = 300(kg/m^3)
$A_s = A'_s = 6\Phi_{10}$
R=4

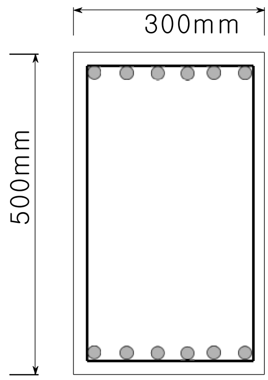

Fig. 13 Time -variant interaction diagrams for XS1 class. A nominal scenario is assumed with prescriptive limits for 50 years expected life, except for w_c, assumed 0.45 (case 9)

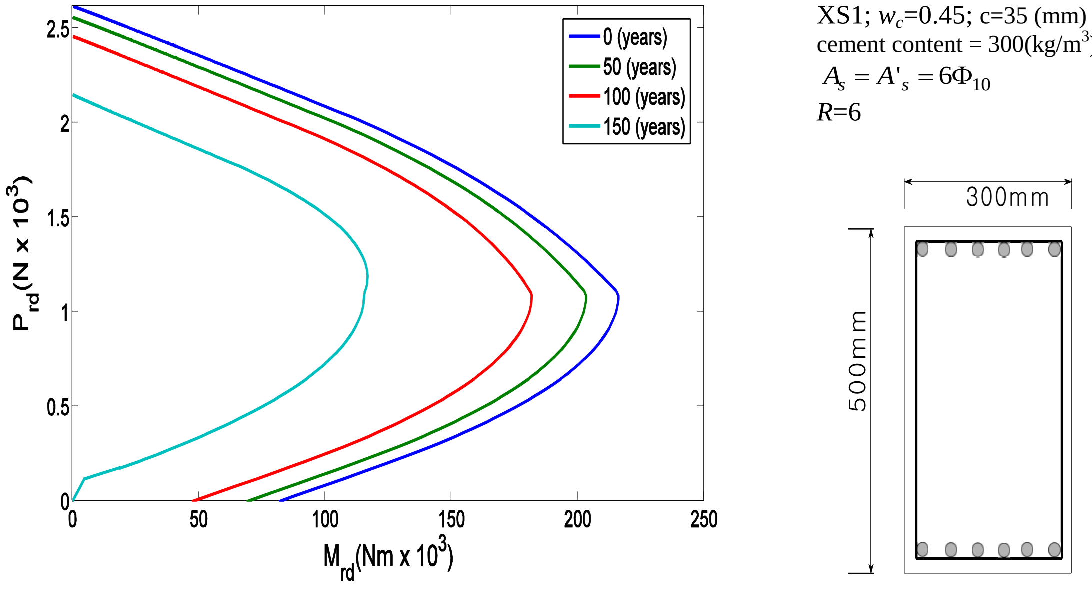

Case 10
XS1; w_c=0.45; c=35 (mm)
cement content = 300(kg/m^3)
$A_s = A'_s = 6\Phi_{10}$
R=6

Fig. 14. Time -variant interaction diagrams for XS1 class.. A nominal scenario is assumed with prescriptive for 50 years expected life, except for w_c, assumed 0.45 (case 10)

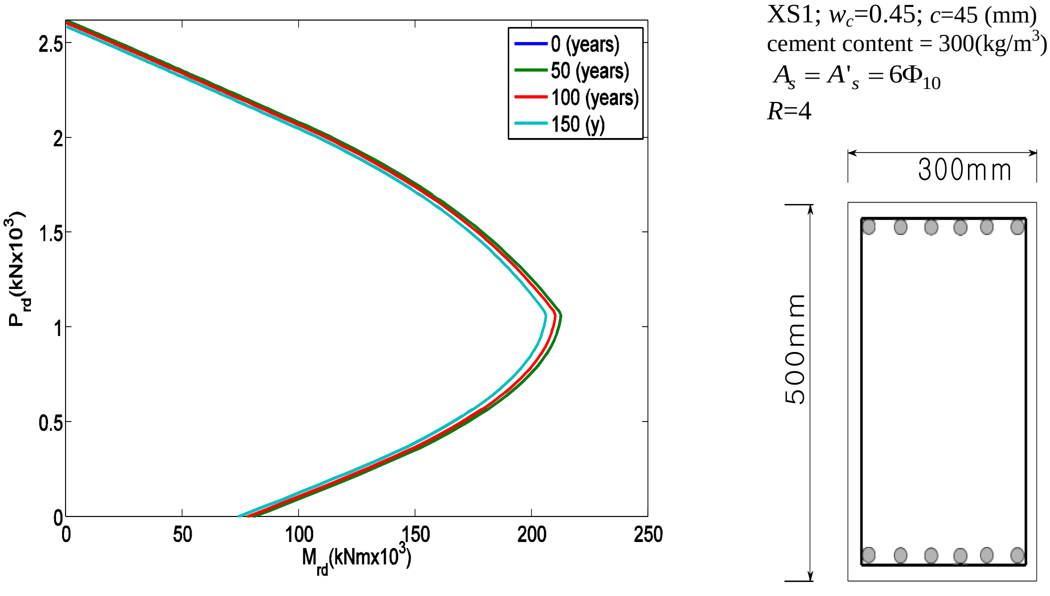

Case 11
XS1; w_c=0.45; c=45 (mm)
cement content = 300(kg/m^3)
$A_s = A'_s = 6\Phi_{10}$
R=4

Fig. 15. Time -variant interaction diagrams for XS1 class. A nominal scenario is assumed with prescriptive limits for 100 years expected life, except for w_c, assumed 0.45 (case 11)

Analogously, comparing Figs. 10 and 14 it is noticed that for w_c=0,45 the column shows a lower strength deterioration.

If the value w_c =0,45 ratio is adopted in the exposure class XS1 for a minimum concrete cover of 45 mm, the load carrying column capacity is practically the same after 100 years, without any reduction over the overall lifetime (see Fig. 15).

From the results of the cases of study developed for the XS1 exposure class, one can conclude that prescriptive limits for 50 and 100 years are insufficient to guarantee structural performances over these target lifetimes. In particular, the minimum concrete cover prescribed for 50 years lifetime should be increased to guarantee unchanged performance over this target lifetime. In fact, only the minimum concrete cover prescribed for 100 years lifetime seems to be adequate to assure constant load carrying capacity of the columns over 50 years lifetime. Moreover, also the maximum water/cement ratio seems to be inadequate for this exposure class, especially when a high pitting factor can be presumed.

Finally, the influence of the bars diameter suggests as an interesting point to give some prescriptions on minimum diameters in relation to the aggressive scenario and pitting factor.

Fig. 16 shows time -variant interaction diagrams for the RC column in the exposure class XS2. A nominal aggressive scenario has been considered and prescriptive limits given for a target lifetime of 50 years. First, the case of $A_s = A'_s = 4\Phi_{12}$ and R=4 has been considered. As for the previous examined exposure class, it is observed that prescriptive limits for this exposure class do not assure that the column strength is guarantee during the target lifetime. The reduction of the strength in terms of ultimate bending at the balanced rupture is of 4,69 % after 50 years and of the 10,42% after 100 years. The reduction of the strength over the time increases as the pitting factor increases and the bars diameters decreases (Fig. 17). As for the XS1 class, also for the class XS2 it would be desirable to increase minimum concrete cover.

In the case of study examined in Fig. 18, the column is supposed designed according to prescriptive limits for a target lifetime of 100 years. The other data are the same of the case examined in Fig. 17. A reduction of column strength is observed with respect to the case examined in Fig. 17, even if it is noticed that these limits are far from ensuring the target lifetime of 100 years for the column. In order to further reduce the strength deterioration it would be necessary to reduce the w_c ratio. Fig. 19 shows the interaction diagrams for the same case of Fig. 18 but adopting w_c=0.4. One observes that the column degrades lesser over the time (Fig. 19). Figs. 20-23 show time variant interaction diagrams for the RC column in the exposure class XS3. In Fig. 20, the nominal aggression scenario and the prescriptive limits given for a target lifetime of 50 years have been considered. The reinforcement is made by $A_s = A'_s = 4\Phi_{12}$. As for the previous examined exposure classes it is observed that prescriptive limits for 50 years exposure class do not assure that the column strength is guarantee during the target lifetime. The reduction of the strength in terms of ultimate bending at the balanced rupture is 1,4% after 50 years and 4,1% after 100 years.

In the case of study examined in Fig. 21, the column is supposed designed according to prescriptive limits for a target lifetime of 100 years. The other data are the same of the example in Fig. 20. A reduction of column strength is observed with respect to the case examined in Fig. 20. The reduction of the column strength over the time increases as the pitting factor increases and the bars diameters decreases (Fig. 22).

Case 12
XS2; w_c=0.45; c= 40(mm)
Cement content = 320(kg/m^3)
$A_s = A'_s = 4\Phi_{12}$
R=4

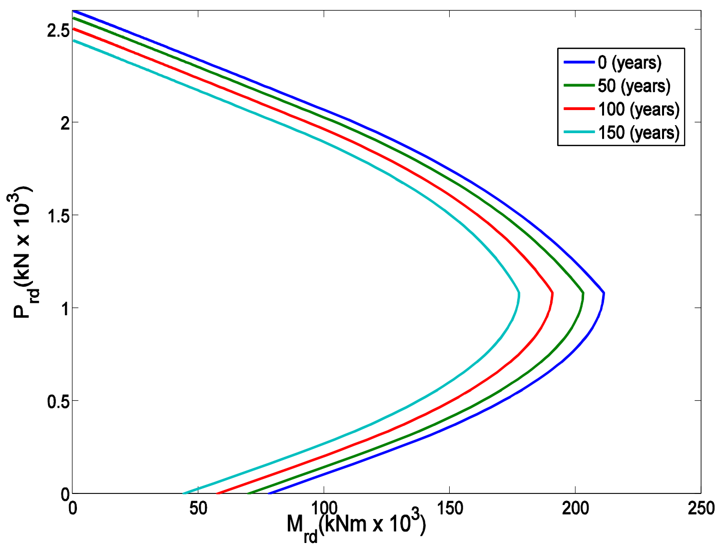

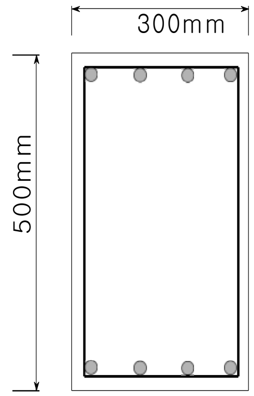

Fig. 16 Time -variant interaction diagrams for XS2 class. A nominal scenario is assumed with prescriptive limits for 50 years expected life (case 12)

Case 13
XS2; w_c=0.45; c= 40(mm)
cement content = 320(kg/m^3)
$A_s = A'_s = 6\Phi_{10}$
R=6

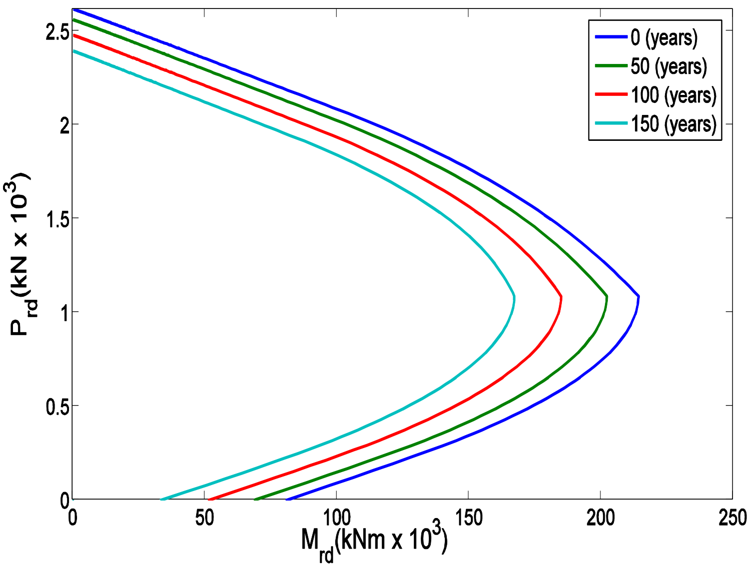

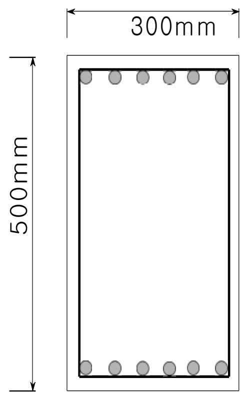

Fig. 17 Time -variant interaction diagrams for XS2 class. A nominal scenario is assumed with prescriptive limits for 50 years expected life (case 13)

Case 14
XS2; w_c=0.45; c=50 (mm)
cement content = 320(kg/m^3)
$A_s = A'_s = 6\Phi_{10}$
R=6

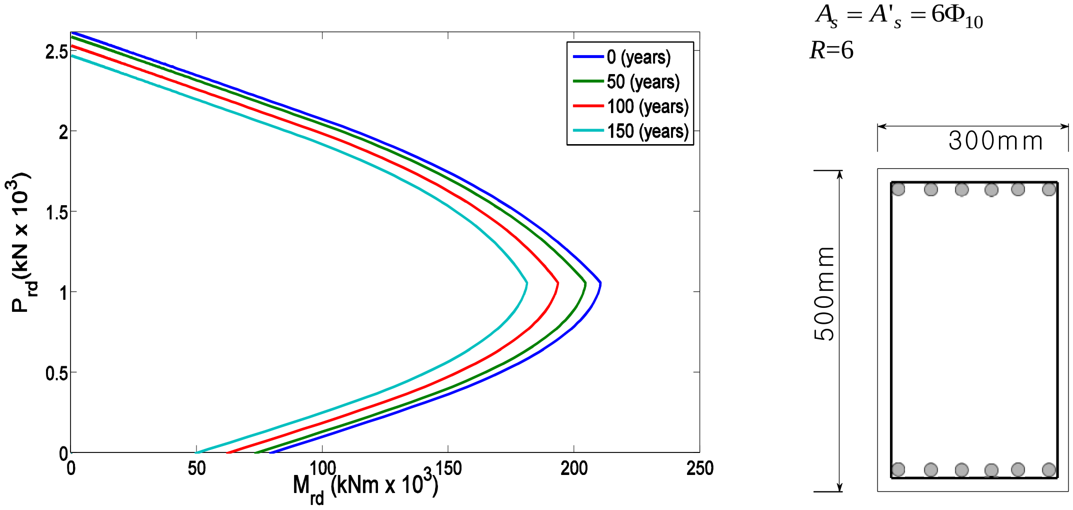

Fig. 18 Time -variant interaction diagrams for XS2 class. A nominal scenario is assumed with prescriptive limits for 100 years (case 14)

Case 15
XS2; w_c=0.40; c= 50(mm)
cement content = 320(kg/m^3)
$A_s = A'_s = 6\Phi_{10}$
R=6

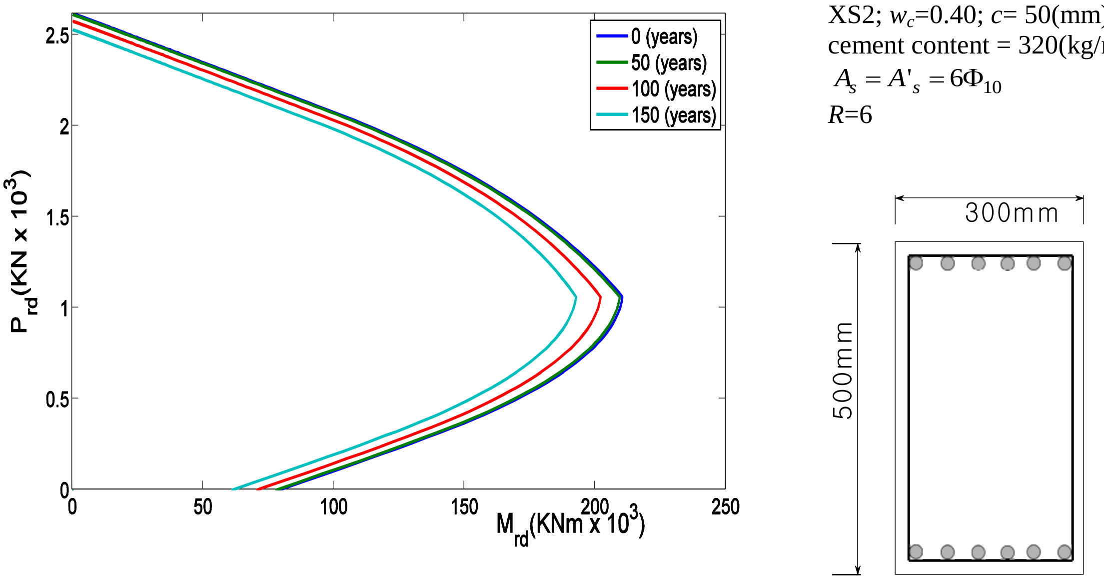

Fig. 19 Time -variant interaction diagrams for XS2 class. A nominal scenario is assumed with prescriptive limits for 100 years expected life except for w_c=0.4 (case 15).

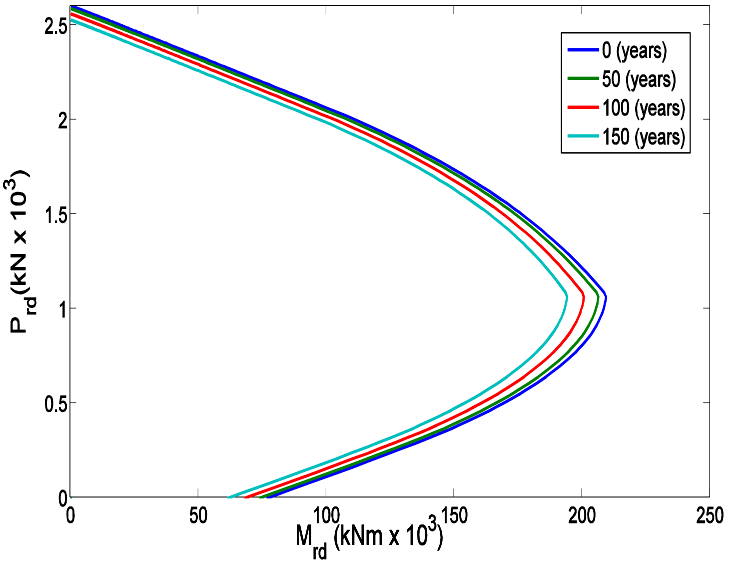

Case 16

XS3; w_c = 0.45; c = 45 (mm)

cement content = 340(kg/m^3)

$A_s = A'_s = 4\Phi_{12}$

R = 4

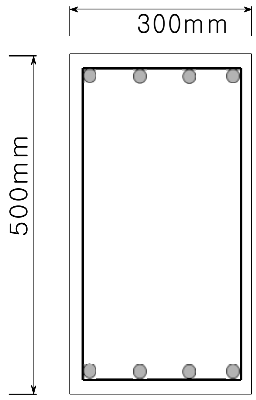

Fig. 20 Time -variant interaction diagrams for XS3 class. A nominal scenario is assumed with prescriptive limits for 50 years expected life (case 16)

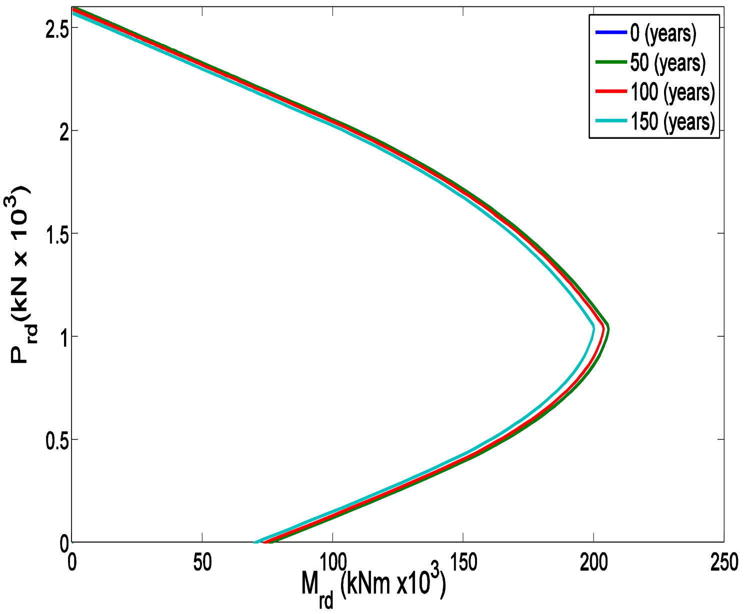

Case 17

XS3; w_c = 0.45; c= 55 (mm)

cement content = 340(kg/m^3)

$A_s = A'_s = 4\Phi_{12}$

R = 4

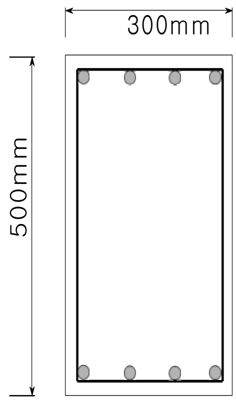

Fig. 21 Time -variant interaction diagrams for XS3 class. A nominal scenario is assumed with prescriptive limits for 100 years expected life (case 17)

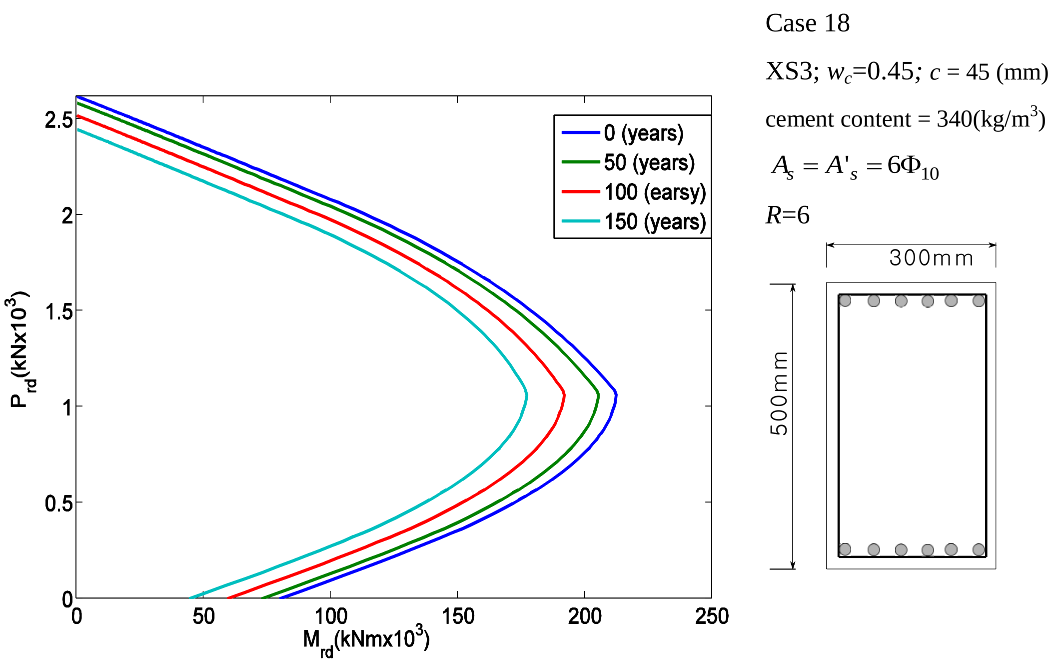

Fig. 22 Time -variant interaction diagrams for XS3 class. A nominal scenario is assumed with prescriptive limits for 50 years expected life (case 18)

Table 6 Ultimate bending at the balanced rupture M_{rdb}, ultimate bending M_{rd} in the case of simple bending, ultimate axial force N_{rd} in the case of simple compression at t=0 years

	t = 0 years		
Case of study	M_{rdb}(KNmx10^3)	M_{rd} (KNmx10^3)	N_{rd}(KNx10^3)
1 (Fig.5)	212,90	78,68	2.60
2 (Fig.6)	212,90	78,68	2,60
3 (Fig.7)	212,90	78,68	2,60
4 (Fig.8)	209,2	77,05	2,60
5 (Fig.9)	216,9	82,00	2,61
6 (Fig.10)	216,9	82,00	2,61
7 (Fig.11)	265,2	133,14	2,84
8 (Fig.12)	212,9	78,68	2,60
9 (Fig.13)	216,9	82,00	2,61
10 (Fig.14)	216,9	82,00	2,61
11 (Fig.15)	212,90	78,68	2,61
12 (Fig.16)	212,90	78,68	2,60
13 (Fig.17)	216,9	82,00	2,61
14 (Fig.18)	210,4	78,52	2,61
15 (Fig.19)	216,9	78,52	2,61
16 (Fig.20)	209,2	77,05	2,60
17 (Fig.21)	205,5	75,47	2,60
18 (Fig.22)	212,3	79,65	2,61

Table 7 Ultimate bending at the balanced rupture M_{rdb}, ultimate bending M_{rd} in the case of simple bending and ultimate axial force N_{rd} in the case of simple compression and % of loss of steel area at t=50 years

Case of study	t = 50 years			
	M_{rdb}(KNmx10^3)	M_{rd} (KNmx10^3)	N_{rd} (KNx10^3)	As loss %
1 (Fig.5)	204,09 (3,65%)	70,18 (10,79%)	2,56 (1,44%)	10,55%
2 (Fig.6)	204,00 (3,89%)	71,25 (9,43%)	2,56 (1,45%)	10,64%
3 (Fig.7)	199,01(6,5%)	64,78 (17,66%)	2,53 (2,45%)	18,02%
4 (Fig.8)	207,1(1,00%)	73,14 (5,07%)	2,58(0,75%)	5,15%
5 (Fig.9)	204,10 (5,9%)	68,84 (14,82%)	2,56 (2,09%)	14,83%
6 (Fig.10)	196,3 (9,5%)	62,12 (24,24%)	2,52 (3,54%)	25,08 %
7 (Fig.11)	254,4 (4,0%)	120,56 (9,44%)	2,79 (1,77%)	8,44 %
8 (Fig.12)	208,0 (2,3%)	72,57 (7,75%)	2,57 (1,06%)	7,79 %
9 (Fig.13)	208,0 (4,1%)	72,80 (11,22%)	2,57 (1,55%)	11,01%
10 (Fig.14)	203,3 (6,2%)	66,94 (18,36%)	2,54 (2,65%)	18,78%
11 (Fig.15)	212,8 (0%)	78,68 (0%)	2,61 (0%)	0%
12 (Fig.16)	202,9(4,69%)	69,91 (11,14%)	2,56 (1,52%)	11,16%
13 (Fig.17)	202,1 (6,82%)	69,45 (15,30 %)	2,56 (2,21 %)	15,68 %
14 (Fig.18)	204,3 (2,8%)	72,37 (7,8%)	2,58 (1,16 %)	8,25 %
15 (Fig.19)	215,7 (0,5%)	77,97 (0,7%)%)	2,61 (0.2%)	1,49 %
16 (Fig.20)	206,2 (1,4%)	73,79 (4,2%)	2,59 (0.51%)	3,78%
17 (Fig.21)	205,5 (0%)	75,47 (0%)	2,60 (0%)	0%
18 (Fig.22)	205,2 (3,34%)	72,27(9,27%)	2,58 (1,31%)	9,3%

Table 8 Ultimate bending at the balanced rupture M_{rdb}, ultimate bending M_{rd} in the case of simple bending and ultimate axial force N_{rd} in the case of simple compression and % of loss of steel area at t=100 years

Case of study	t = 100 years			
	M_{rdb}(Nmx10^3)	M_{rd} (Nmx10^3)	N_{rd}(Nx10^3)	As loss %
1 (Fig.5)	192,6 (9,53%)	58,34 (25,84%)	2,50 (3,64%)	26,71%
2 (Fig.6)	192,40 (9,62%)	58,30 (25,90%)	2,50 (3,65%)	26,82 %
3 (Fig.7)	179,21 (15,82%)	45,37 (42,33%)	2,44 (5,99%)	43,98 %
4 (Fig.8)	200 (4,3%)	65,45 (15,05%)	2,54 (2,12%)	15,65%
5 (Fig.9)	187,01 (13,78%)	52,58 (35,87%)	2,48 (5,19%)	36,78 %
6 (Fig.10)	169,4 (21,8%)	34,79 (57,57%)	2,40 (8,33%)	59,01%
7 (Fig.11)	237,5 (10,4%)	102,56 (22,96_%)	2,71 (4,55%)	21,61%
8 (Fig.12)	197,8 (7,1%)	62,82 (20,14%)	2,53 (2,76%)	20,27%
9 (Fig.13)	194,5 (10,32%)	59,87(26,98%)	2,51 (3,97%)	28,14 %
10 (Fig.14)	181,7 (16,2%)	45,03 (45,07%)	2,44 (6,51%)	46,17 %
11 (Fig.15)	209,9 (1,13%)	77,42 (2,97%)	2,60 (0,43%)	3,08%
12 (Fig.16)	190,7 (10,42%)	57,09 (27,43 %)	2,50 (3,76 %)	27,61%
13 (Fig.17)	185,00 (14,7 %)	51,76 (36,88 %)	2,47 (5,3 %)	37,97 %
14 (Fig.18)	193,4 (8,0%)	62,18 (20,81%)	2,53 (3,27 %)	23,18 %
15 (Fig.19)	204,5 (5,7%)	72,74 (7,35%)	2,58 (1,33%)	9,42%
16 (Fig.20)	200,6 (4,1%)	68,47(11,13%)	2,56 (1,55%)	11,43 %
17 (Fig.21)	203,2 (1,1%)	74,40 (1,41%)	2,59 (0,16)	1,17 %
18 (Fig.22)	191,7 (9,7%)	59,19 (25,68%)	2,51 (1,81%)	27,07%

Table 9 Ultimate bending at the balanced rupture M_{rdb}, ultimate bending M_{rd} in the case of simple bending and ultimate axial force N_{rd} in the case of simple compression and % of loss of steel area at t=150 years

Case of study	t = 150 years			
	M_{rdb}(Nmx10^3)	M_{rd} (Nmx10^3)	N_{rd}(Nx10^3)	As loss %
1 (Fig.5)	179,20 (15,82%)	44,93 (42,88%)	2,44 (6,03%)	44,31%
2 (Fig.6)	179,01(15,92%)	44,90 (42,92%))	2,44 (6,05)	44,42 %
3 (Fig.7)	116,00(45%)	-	2,15 (17,34%)	-
4 (Fig.8)	192,1 (8,16%)	56,92 (26,12%)	2,50 (3,72%)	27,33%
5 (Fig.9)	169,10 (21%)	34,48 (57,95%)	2,39 (8,38%)	59,49%
6 (Fig.10)	110,70 (48,0%)	-	2,11 (19,10%)	-
7 (Fig.11)	218,6 (17,5%)	84,94 (36,20%)	2,62 (7,65%)	36,28%
8 (Fig.12)	187,2 (14,9%)	52,55 (33,20%)	2,48 (4,67 %)	34,26%
9 (Fig.13)	179,8 (17,1%)	44,54(45,67%)	2,44 (6,58%)	46,68%)
10 (Fig.14)	116,7 (46,0%)	-	2,14 (18,17%)	-
11 (Fig.15)	205,4 (3,25%)	73,52 (7,69%)	2,58 (1,17%)	8,31%
12 (Fig.16)	177,5 (16,62 %)	43,96 (44,12 %)	2,44 (6,18 %)	45,42 %
13 (Fig.17)	167,2 (22,91 %)	33,56 (59,06%)	2,39 (8,58 %)	60,86%
14 (Fig.18)	181,1 (13,0%)	49,60(36,82%)	2,47 (5,62%)	39,82 %
15 (Fig.19)	194,6 (10,2 %)	64,50 (17,85%)	2,54(/2,7%)	19,56 %
16 (Fig.20)	194,0 (7,2%)	62,40 (19,01%)	2,53 (2,79%)	20,46 %
17 (Fig.21)	199,9 (2,7%)	70,99 (5,93%)	2,58 ()0,8%)	5,88 %
18 (Fig.22)	176,7 (16,7%)	44,49 (44,11%)	2,44 (6,5%)	46,56%

From the results of the cases of study developed for the XS2 and XS3 exposure classes, therefore one can confirm the same conclusions carried out for the class XS1. Moreover, results show that prescriptive limits for class XS3 seem more adequate than rules assigned for classes XS2 and XS1.

7. Conclusions

Corrosion of steel rebar is the most common cause of deterioration of RC members. It is the primary state that limits the service life of concrete structures, particularly, in severe environments such as marine ones. This paper presents a strength deterioration evaluation method for RC columns exposed to chloride pitting attack in marine environments, obtaining time-variant axial-bending interaction diagrams. The initiation and propagation model is elaborated for XS exposure classes, assigning the admissible minimum values of concrete cover and cement content, and the maximum value of w_c ratio prescribed for each class. Moreover, critical chloride concentration and chloride surface concentration are assumed according to literature data for the selected classes.

The results obtained show that for all exposure classes, prescriptive limits for 50 and 100 years are unable to guarantee structural performances over these target lifetimes. More in detail, the minimum concrete cover prescribed for 50 years lifetime is insufficient and therefore it should be increased to guarantee unchanged performance over this target lifetime. Moreover, also the maximum water/cement ratio seems to be inadequate, especially when a high pitting factor can be presumed. The relevance of the bars diameter on the strength deterioration suggests as an interesting point to give some prescriptions on minimum diameter in relation to the aggressive scenario and pitting factor. Moreover, results show that prescriptive limits for class XS3 seem more adequate than rules assigned for classes XS2 and XS1. The proposed model furnishes a good quantitative estimate of the remaining strength of corroded concrete columns members, which helps in establishing design details.

Acknowledgments

This research was founded by the research project \DPC-243 ReLUIS 2014, RS 11 "Trattamento delle incertezze nella valutazione degli edifci esistenti"

Rererences

ACI (American Concrete Institute) (2008), *ACI 318-08: Building Code Requirements for Structural Concrete*, ACI, Farmington Hills, MI, USA.

Amey, S.L., Johnson, D.A., Miltenberger, M.A. and Farzam, H. (1998), "Predicting the service life of concrete marine structures: an environment methodology", *ACI Struct. J.*, **95**(2), 205–214.

Andrade, C., Tavares, F., Castellote, M., Petre-Lazars, I., Climent, M.A. and Vera, G. (2006), "Comparison of chloride models: the importance of surface condition", *In: Second international symposium on advances in concrete through science and engineering*, Quebec City, Canada.

Andrade, C., Prieto, M., Tanner, P., Tavares, F. and Andrea, R. (2013), "Testing and modelling chloride penetration into concrete", *Constr. Build. Mater.*, **39**, 9-18.

Bamforth, P.B. and Price, W.F. (1997), *An International Review of Chloride Ingress into Structural Concrete*, Transport Research Laboratory report 359, Scotland.

Cheewaket, T., Jaturapitakkul, C. and Chalee, W. (2013), "Concrete durability presented by acceptable chloride level and chloride diffusion coefficient in concrete: 10-year results in marine site", *Mater. Struct.*, DOI 10.1617/s11527-013-0131-4.

Costa, A. and Appleton, J. (1999), "Chloride penetration into concrete in marine environment-Part II: Prediction of long term chloride penetration", *Mater. Struct.*, **32,** 354-359.

Crank, J. (1975), *The mathematics of diffusion. 2nd ed*, London, Oxford.

Dousti, A., Shekarchi, M., Alizadeh, R. and Taheri, A. (2011), "Binding of externally supplied chlorides in micro silica concrete under field exposure conditions", *Constr. Build. Mater.*, **33**, 1071-1079.

EN 206-1, (2001), *Concrete-Part 1: Specification, Performance, Production and Conformity*, European standard, Berlin, Germany.

Hooton, R.D., Geiker, M.R. and Bentz, E.C. (2002), "Effects of curing on chloride ingress and implications on service life, *ACI Mater. J.*, **99**, 201–206.

Kassir, M.K. and Ghosn, M. (2002), "Chloride-induced corrosion of reinforced concrete bridge decks", *Cement Concrete Res.*, **32**, 139–143.

Kropp, J. (1995), *Chlorides in Concrete. In: Performance Criteria for Concrete Durability*, RILEM Report 12, E& FN SPON, 138–164.

Lau, K., Powers, R.G. and Sagues, A.A. (2006), "Corrosion performance of concrete cylinder piles", *In: 61th NACE conference on corrosion*, Houston, USA.

Mangat, P.S. and Molloy, B.T. (1994), "Prediction of long-term chloride concentration in concrete", *Mater. Struct.*, **27**, 338-346.

Mehta, P.K. (1988), "Durability of concrete exposed to marine environment- fresh look", *ACI SP 109*, 1-29.

Model code-fib, (2011), fib Special Activity Group 5.

Moodi, F., Ramezanianpour, A.A. and Jahangiri, E. (2014), "Assessment of some parameters of corrosion initiation prediction of reinforced concrete in marine environments", *Comput. Concr.*, **13**(1).

Moradllo, M., Shekarchi, M. and Hoseini, M. (2012), "Time-dependent performance of concrete surface coatings in tidal zone of marine environment", *Constr. Build. Mater.*, **30**(1), 198-205.

Nilsson, L.O. (2006), "Present limitations of models for predicting chloride ingress into reinforced concrete structures", *J. Phys. IV France*, **136**, 123–130.

Nokken, M., Boddy, A., Hooton, R.D. and Thomas, M.D.A. (2006), "Time dependent diffusion in concrete-three laboratory studies", *Cement Concrete Res.*, **36,** 200-207.

Pack, S., Jung, M., Song, H., Kim, S. and Ann, K.Y. (2010), "Prediction of time dependent chloride transport in concrete structures exposed to a marine environment", *Cement Concrete Res.*, **40,** 302-312.

Petcherdchoo, A. (2013), "Time dependent models of apparent diffusion coefficient and surface chloride for chloride transport in fly ash concrete", *Constr. Build. Mater.*, **38**, 497-507.

Ramezanianpour, A.A., Jahangiri, E., Ahmadi, B. and Moodi, F. (2012), "Evaluation and modification of the fib service-Life design model for the Persian Gulf region", *In: fib symposium: concrete structures for sustainable community*, Stockholm, Sweden.

Ramezanianpour, A.A. and Pourkhorshid, A.R. (2012), "Durable concretes for hot and severe environments", *In: International congress on durability of concrete*, Trondheim, Norway.

Rilem report 14, (1996), Durability design of concrete structures, *In: Sarja A, Vesikari E, editors*, E&FN Spon.

Saassouh, B. and Lounis, Z. (2012), "Probabilistic modeling of chloride-induced corrosion in concrete structures using first and second-order reliability methods", *Cement Concrete Compos.*, **34**, 1082–1093.

Safehian, M. and Ramezanianpour, A.A. (2013), "Assessment of service life models for determination of chloride penetration into silica fume concrete in the severe marine environmental condition", *Constr. Build. Mater.*, **48**(1), 287-294.

Safehian, M. and Ramezanianpour, A.A. (2014), "Assessment of long term chloride diffusion in real RC structures in marine environment", *European J.Sci. Res.*, **120**(3), 332-345.

Shekarchi, M., Alizadeh, R., Ghods, P., Chini, M. and Hosseini, M. (2008), "Durability based design of RC structures in south of Iran using DuraPGulf model", *AJSE, Arabian J.Sci. Eng.*, **33**(1), 77–88.

Shekarchi, M., Moradi, F. and Pargar, F. (2011), "Study on corrosion damage of a reinforced concrete jetty structure in coastal region of Persian Gulf, a case Study", *Struct. Infrastr. Eng.*, **7**(9), 701-713.

Shin, K.J., Kim, J.S. and Lee, K.M., (2011), "Probability-based durability design software for concrete structures subjected to chloride exposed environments", *Comput. Concr.*, **8**(5).

Stanish, K. and Thomas, M.D.A. (2003), "The use of bulk diffusion tests to establish time-dependent concrete chloride diffusion coefficients", *Cement Concrete Res.*, **33**, 55-62.

Tang, L. and Gulikers, J. (2007), "On the mathematics of time-dependent apparent chloride diffusion coefficient in concrete", *Cement Concrete Res.*, **37**, 589-595.

Thomas, M.D.A. and Bentz, E.C. (2001), "Life 365: Computer program for predicting the service life and life-cycle costs of reinforced concrete exposed to chlorides", *Am. Concrete Inst.*, Committee 365, Service life prediction, Detroit, Michigan.

Tuutti, K. (1996), "Chloride induced corrosion in marine concrete structures", *In: Durability of concrete on saline environment*, Uppsala; 81-93.

Vennesland, Q., Climent, M.A. and Andrade, C. (2013), "Recommendation of RILEM TC 178-TMC: Testing and modelling chloride penetration in concrete", *Mater. Struct.*, **46**, 337-344.

Wang, X.Y., Park, K.B. and Lee, H.S. (2012), "Modeling of chloride diffusion in a hydrating concrete

incorporating silica fume", *Comput*. *Concr*., **10**(5).
Yuan, Q., Shi, C., Schutter, G.D., Audenaert, K. and Deng, D. (2009), "Chloride binding of cement-based materials subjected to external chloride environment-A review", *Constr*. *Build*. *Mater*., **23**(1), 1-13.
Zhang, S., Lu, C. and Liu, R. (2011), "Experimental determination of chloride penetration in cracked concrete beams", *Procedia Eng*., **24**, 380-384.

CC